Gallium-68 citrate PET/CT findings in an experimental model of acute appendicitis in rabbits

Aziz Gültekin (agultekin@pau.edu.tr)
Pamukkale University, Medical Faculty https://orcid.org/0000-0002-0311-8077
Osman Uzunlu
Pamukkale University
Ayşe Uğur
Pamukkale University
Neşe Demirkan
Pamukkale University
Esin Avcı
Pamukkale University
Doğangün Yüksel
Pamukkale University

Original research

Keywords: Acute appendicitis, Gallium 68-citrate, PET/CT, Interleukin-6, Procalcitonin

Posted Date: March 11th, 2020

DOI: https://doi.org/10.21203/rs.3.rs-16741/v1

Title

Gallium-68 citrate PET/CT findings in an experimental model of acute appendicitis in rabbits.

Short title

^{68}Ga citrate PET/CT in appendicitis

Authors

Aziz Gültekin[1*], Osman Uzunlu[2], Ayşe Uğur[3], Neşe Demirkan[4], Esin Avcı[5] and Doğangün Yüksel[1]

Affiliations

[1] Pamukkale University Medical Faculty, Departmant of Nuclear Medicine, Denizli, Turkey.

[2]Pamukkale University Medical Faculty, Departmant of Pediatric Surgery, Denizli, Turkey.

[3] Pamukkale University, Education and Research Hospital, Departmant of Nuclear Medicine, Denizli, Turkey.

[4] Pamukkale University Medical Faculty Departmant of Pathology, Denizli, Turkey.

[5] Pamukkale University Medical Faculty Departmant of Biochemistry, Denizli, Turkey.

*__Correspondence should be addressed to Aziz Gültekin__ Pamukkale University Medical Faculty, Departmant of Nuclear Medicine, Denizli, Turkey, e-mail: agultekin@pau.edu.tr, phone: +905054969348, fax: +90 258 296 6001,

Funding The study was supported financially by the Scientific Research Projects (BAP) of Pamukkale University, Denizli-Turkey.

Gallium-68 citrate PET/CT findings in an experimental model of acute appendicitis in rabbits

Abstract

Objective Acute appendicitis (AA) is the most common abdominal surgical emergency worldwide. Several infection and inflammation imaging methods have been used in a limited number of cases. Gallium-68 (^{68}Ga) has recently been investigated as an infection and inflammation imaging agent. The aim of our study was to produce ^{68}Ga-citrate in an automated synthesis unit and perform ^{68}Ga-citrate PET/CT imaging in rabbits with experimentally induced AA. Furthermore, this study aimed to investigate and correlate PET/CT findings with those of histopathological and biochemical examinations.

Methods ^{68}Ga-citrate was synthesized using the cationic method in an automatic synthesis unit. Twelve rabbits of the New Zealand strain (*Oryctolagus cuniculus*) were divided into two groups. In the AA group (n = 6), the appendices of the rabbits were surgically ligated. In the sham group (n = 6), the abdomen was surgically opened and closed. All rabbits were imaged using ^{68}Ga-citrate PET/CT at 12, 24 and 36 h following the establishment of the experimental models, and at 36 h, all rabbits were appendectomised. Appendices were examined histopathologically and blood samples were drawn from all rabbits at the beginning and end of the experimental process. Interleukin-6 (IL-6) and procalcitonin (Pct) levels were measured. PET/CT results were compared statistically with histopathological and biochemical references.

Results The labelling efficiency of ^{68}Ga-citrate was more than 98%. The sensitivity, specificity and accuracy of ^{68}Ga-citrate PET/CT in AA were 100%, 83.3% and 81.7%, respectively. IL-6 and Pct levels at 36 h in the AA group were significantly higher than those in the sham group and at baseline ($p < 0.05$).

Conclusions ^{68}Ga-citrate was synthesized in an automatic synthesis unit for the first time, and ^{68}Ga-citrate uptake was shown using PET/CT in a histopathologically and biochemically confirmed experimental AA rabbit model.

Keywords Acute appendicitis, Gallium 68-citrate, PET/CT, Interleukin-6, Procalcitonin

Introduction

Acute appendicitis (AA) is the most common emergency surgical condition. The annual incidence of AA in developed countries is 100–140 per 100,000 individuals [1]. The lifetime risk of AA is approximately 6.7%–8.6% [2]. The clinical characteristics of AA can range from mild symptoms to fatal conditions such as peritonitis and sepsis. Its diagnosis can be occasionally very difficult. The primary treatment approach is surgery [3]. Mortality rates post appendectomy are very low in patients without perforation (0.07%–0.7%) and may vary between 0.5% and 2.4% in perforated cases [4]. It is important to distinguish between complicated and uncomplicated AA. Although computed tomography (CT) is successful in making this distinction, it may be inadequate [5,6]. The main purpose of diagnostic methods used in AA is to reduce hospital costs and labour loss by simultaneously reducing the rates of negative laparotomy and perforated appendicitis [7]. In fact, reliable imaging methods in patients with suspected appendicitis may reduce the rate of negative appendectomies by almost 15% [8]. Currently, there is no ideal diagnostic tool that can be used alone to provide a definite and accurate diagnosis before surgery. Research efforts to find and introduce non-invasive, inexpensive and practically usable laboratory methodologies that do not depend on the user's experience in the diagnosis of AA are still ongoing [13]. AA is a well-known infection and inflammation. Thus, nuclear infection and inflammation imaging methods are rarely performed for AA. Previous studies have reported the use of Indium-111 and ^{99m}Tc-HMPAO-labelled leukocyte scintigraphy, ^{99m}Tc-labelled human immune globulin and anti-granulocyte antibodies in AA cases [10,11]. In recent years, incidental cases of AA have been identified during ^{18}F-FDG PET/CT scans for oncologic screening [12-15]. One of the most popular agents used for infection and inflammation nuclear imaging is Gallium-67 (^{67}Ga), which has been used for imaging purposes for the past 40 years [16]. However, ^{67}Ga is not a convenient molecule for the clinical management of AA, which is an emergency surgical condition, because of its distinct disadvantages. Recently, the widespread use of ^{68}Ge/^{68}Ga generators has suggested that Ga-labelled radiopharmaceuticals can be used for infection and inflammation imaging. For this purpose, ^{68}Ga-citrate has been most commonly labelled and used to display infection and inflammation in pre-clinical and clinical trials [17,18]. Various biochemical examinations have been performed for the diagnosis of AA, and the most useful tests included

leukocyte count and C-reactive protein level measurement [19,20]. However, the contribution of other acute-phase reactants, such as D-dimer, IL-2, IL-6 and Pct to AA diagnosis has also been investigated. For instance, Pct, IL-6, IL-2 and D-dimer plasma levels are elevated during the course of AA [21-23].

The aim of our study was to investigate the diagnostic ability of ^{68}Ga-citrate PET/CT in experimentally induced AA rabbits.

Materials and methods

^{68}Ga-Citrate labelling and quality control

$GaCl_3$ used for the synthesis of ^{68}Ga-citrate was obtained from ^{68}Ge/^{68}Ga generator in the Scintomics GmbH GRP module 4V synthesis module. Synthesis of ^{68}Ga-citrate was performed using the Scintomics automated synthesis system.
$GaCl_3$, eluted (925 MBq) from the PSH^+ cartridge with 5.0 M (1.5 ml) NaCl, was added to a borosilicate reaction vial containing dissolved citric acid/trisodium citrate buffer (500 μL, 0.1 M). The product solution was set to a pH value of 4.5 to prevent the formation of $^{68}Ga(OH)_3$ at higher pH values. The mixture was then heated for 10 min at 70°C to label the citrate with $^{68}GaCl_3$. Then, the labelling product was filtered into the product vial through a 0.2 micron membrane filter.

The radiochemical purity of ^{68}Ga-citrate solution was analysed using the Scintomics 8100 radio-high-performance liquid chromatography (HPLC) system equipped with a radioactivity detector. The system maintained a flow rate of 0.5 mL/min and a column temperature of 30°C under experimental conditions. An isocratic separation was then performed using a mobile phase that included acetonitrile (30%) and trifluoroacetic acid (TFA, 0.1 %) in water at a pH of 4.5. The injection volume was 20 μL, and the detection time was determined to be 15 min. Finally, the samples were monitored using a UV detector at 220 nm and a radio-detector to identify potential chemical impurities.

Animal experiments

This prospective study was conducted after obtaining ethical approval from the Animal Experiments Ethics Committee (Jan 11, 2019-60758568-020/2717). European Union directives were complied with. The gender of the animal was not considered to be a factor in the experimental design. All rabbits were cared for, kept in separate cages with 12-h day and night cycles at 25°C during all procedures and fed ad libitum. Twelve New Zealand rabbits (*Oryctolagus cuniculus*) that weighed 2100–2950 g were divided into two groups: AA (n = 6) and sham (n = 6). In all rabbits, ketamine 35 mg/kg (Ketasol 10 mL, Richter Pharma AG, Wels -Australia) and xylazine 5 mg/kg (Rompun 25 mL, Bayer, Turkey) were injected intramuscularly to induce general anaesthesia. The AA and sham

models were established and prepared according to the study performed by Şimşek et al [24]. (Fig. 1) All surgical procedures were performed by an experienced paediatric surgeon with a certificate of experimental animal use.

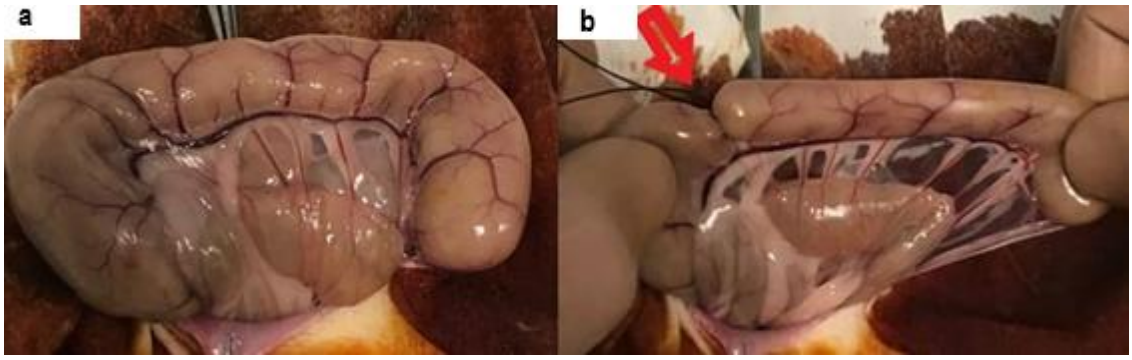

Fig. 1 Establishment of the sham (a) and experimental models of AA (b). The red arrow indicates the region where the appendix was ligated.

^{68}Ga citrate PET/CT imaging and evaluation

All rabbits were anaesthetised. ^{68}Ga-citrate was injected into the ear vein of rabbits at a dose of 18 MBq/kg. Following an uptake time of approximately 60 min, acquisitions were conducted in the prone position. In all cases, PET/CT imaging was performed at 12, 24 and 36 h following the establishment of the experimental model. Rabbits were examined using a PET/CT scanner (Gemini TF TOF PET-CT; Philips, Cleveland, OH; 3D mode, slice thickness of 5 mm, 4 × 4 × 22 mm, 256 × 256 matrix, transverse FOV 576 mm and axial FOV 180 mm). Whole-body emission scans were acquired for a duration of 2 min per position without intravenous contrast injection. Transmission images were obtained using low-dose CT (90 mA, 100 kV, 16 CT detectors, and 5-mm slice thickness). Attenuation correction was performed for PET images using a CT map and ordered subsets-expectation maximization algorithm (33 subsets, 3 iterations). Transverse, sagittal and coronal sections (5-mm thickness) were generated from PET/CT fusion images and were evaluated using the Philips Fusion Viewer software (ver. 2.1; Philips Healthcare, Best, The Netherlands).

Furthermore, ^{68}Ga-citrate PET/CT images were blindly evaluated by a nuclear medicine specialist both visually and semi-quantitatively. The reader evaluated 12-, 24- and 36-h images of each case. Finally, the reader was also asked to conclude whether AA was present or not.

Procalcitonin and interleukin-6 examinations

A total of 3 mL of blood was taken from the ear veins of AA and sham rabbits immediately following model establishment (0 h) and just before performing appendectomy (36 h). Consequently, blood samples were allowed to coagulate at a temperature of 4°C for 30 min. After centrifugation, serum samples were stored at −80°C until IL-6 and Pct serum levels were assessed. IL-6 and Pct levels were quantified using competitive inhibition, an enzyme immunoassay method using a commercial ELISA kit (USCN Life Science Inc., Wuhan, China). Intra- and inter-assay were <5% for both analytes.

Appendectomy of rabbits and histopathological examination

Appendectomy was performed under general anesthesia after 36 h of imaging rabbits. Tissues were fixed at 10% formaldehyde solution for 24 h and embedded in paraffin blocks. 4-micrometre-thick tissue sections were taken from each block, stained with hematoxylin–eosin and examined under a light microscope. Histopathological examinations were performed by a single blinded pathologist.

Statistical analysis

Data were analysed using SPSS 24.0 package software (IBM, Armonk, NY, USA). Continuous variables were expressed as mean ± standard deviation, whereas categorical variables were expressed as numbers and percentages. When parametric test assumptions were provided, the significance of the difference between the two means was used to compare independent group differences. On the other hand, when parametric test assumptions were not provided, the Mann–Whitney U test was used to compare independent group differences. Wilcoxon paired two samples tests were also used for intra-group comparisons. A 2 × 2 contingency table with four diagnostic outcomes was constructed based on the final diagnostic results. A value of $P < 0.05$ was considered significant.

Results

Labelling of citrate with ^{68}Ga in an automated synthesis module and quality control

The generator product ^{68}Ga was labelled with a solution of citric acid/trisodium citrate buffer that was prepared at optimum pH and molarity. High yield (20 mci/740 MBq) ^{68}Ga-citrate was obtained using the cationic method without using organic

solvents. The labelling efficiency was found to be >98%, and the automated synthesis was performed within 15 min. The pH of the final product was 4–5.

Nonetheless, it is necessary to perform a quality control (QC) test to assess the diagnostic efficiency and purity of the synthesized ^{68}Ga-citrate. QC was evaluated using HPLC. Furthermore, the validation of the analytic method for the defined chemical and radiochemical purity of ^{68}Ga-citrate was performed according to Q2 (R1) ICH guidelines [25]. Under the chromatographic conditions defined in the experimental section, the average retention times of ^{68}Ga and of ^{68}Ga-citrate were found to be 2.36 min and 3.83 min, respectively, using a radionuclide detector.

^{68}Ga-citrate PET/CT and histopathological findings

During appendectomy, the appendices were evaluated; two cases were suppurative, three cases were perforated, and one case was gangrenous in the AA group. No appendicitis findings were detected in any rabbit in the sham group. The histopathological and ^{68}Ga-citrate PET/CT results of AA and sham rabbits are shown in Table 1 *(36th hour*).

Table 1 The histopathological and ^{68}Ga-citrate PET/CT results of AA and Sham rabbits

Rabbits							^{68}Ga-citrate PET/CT results
	Macroscopic diagnosis	Exudate	FN	Complete necrosis, peritonitis	NI	Pathological diagnosis	
AA1	perforated	+	++	++	++	Appendicitis	Appendicitis
AA2	suppurative	-	++	-	++	Appendicitis	Appendicitis
AA3	suppurative	-	++	-	++	Appendicitis	Appendicitis
AA4	perforated	+	++	++	++	Appendicitis	Appendicitis
AA5	gangrenous	-	+++	+++	+++	Appendicitis	Appendicitis
AA6	perforated	+	++	++	++	Appendicitis	Appendicitis
Sham1	normal	-	-	-	-	Appendicitis (-)	*Appendicitis*
Sham2	normal	-	-	-	-	Appendicitis (-)	Appendicitis (-)
Sham3	normal	-	+	-	+	Appendicitis (-)	Appendicitis (-)
Sham4	normal	-	+	-	+	Appendicitis (-)	Appendicitis (-)
Sham5	normal	-	-	-	+	Appendicitis (-)	Appendicitis (-)
Sham6	normal	-	-	-	-	Appendicitis (-)	Appendicitis (-)

AA: acute appendicitis; FN: focal necrosis; NI: neutrophilic infiltration; (-): no; (+): mild;(++): moderate; (+++): severe

Table 2 demonstrates the histopathological and ^{68}Ga-citrate PET/CT results (*36th hour*). According to these results, the sensitivity, specificity and accuracy of ^{68}Ga-citrate were 100%, 83.3% and 91.7%, respectively.

Table 2 Sensitivity, specificity, PPV and NPV values for ^{68}Ga-citrate PET/CT

Statistics	Results (%)	CI (95%)
Sensitivity	100	54.07–100
Specificity	83.33	35.55–99.58
PPV	85.71	21.09–78.91
NPV	100	50.06–97.29
Accuracy	91.67	61.52–99.79

PPV: positive predictive value; NPV: negative predictive value

When ^{68}Ga-citrate PET/CT images of experimentally induced AA rabbits were examined, appendix swelling and wall thickening were observed (Fig. 2).

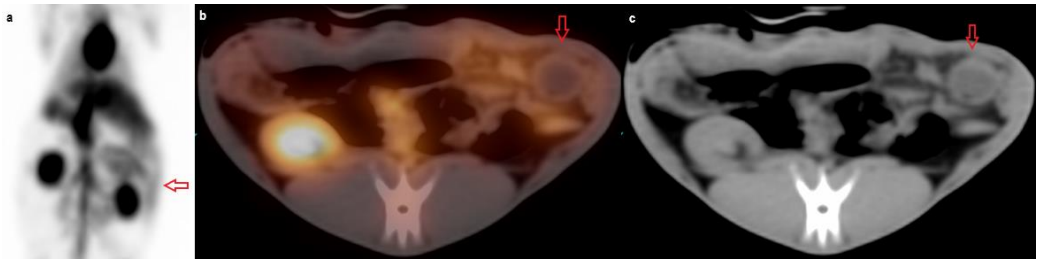

Fig. 2 In 36-h ^{68}Ga-citrate PET/CT images of a rabbit (AA6) with experimental acute appendicitis, acute appendicitis is observed in the abdomen adjacent to the left kidney and spleen. MIP (a); transaxial PET/CT fusion image (b); transaxial CT image (c) (red arrows).

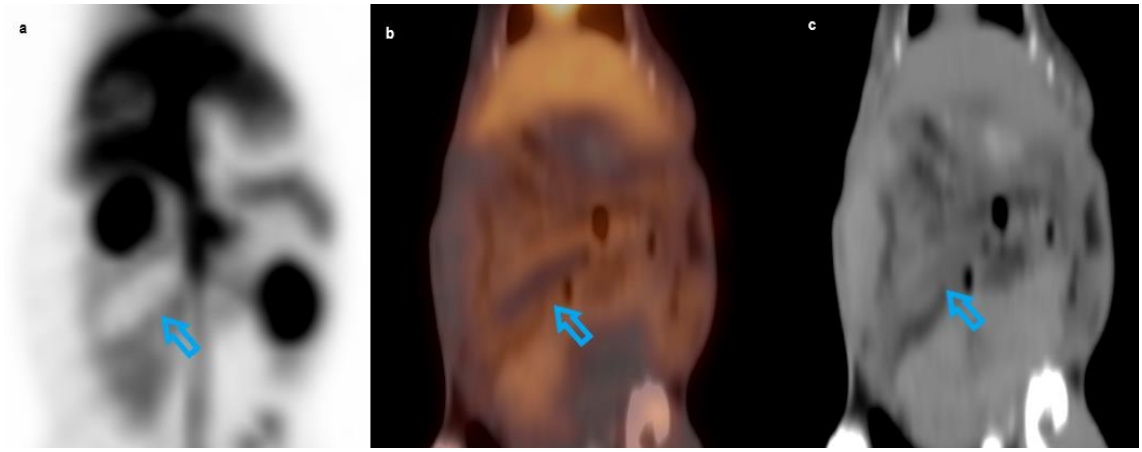

Fig. 3 In 36-h ^{68}Ga-citrate PET/CT images of a rabbit (AA4) with experimental acute appendicitis, acute appendicitis is observed in the abdomen in the right lower quadrant. MIP (a); PET/CT coronal fusion image (b); coronal CT image (c) (blue arrows).

PET also revealed the presence of ^{68}Ga-citrate uptake around this mass starting at 12 h. At 24 and 36 h, ^{68}Ga uptake increased steadily around the appendices. PET/CT accurately demonstrated appendicitis in all rabbits diagnosed with appendicitis histopathologically. All rabbits in the sham group were considered to be pathologically normal, whereas one rabbit in the sham group (sham1) was interpreted as having appendicitis in PET/CT (false positive [FP]). The observer simultaneously performed SUV_{max} measurements when evaluating PET/CT results. The SUV_{max} values measured from the appendix region of all rabbits in the AA group in PET/CT were at a moderate level. However, in all three scans, SUV_{max} values measured from the abdominal region of rabbits in the sham group were lower than those in the AA group (Fig. 4).

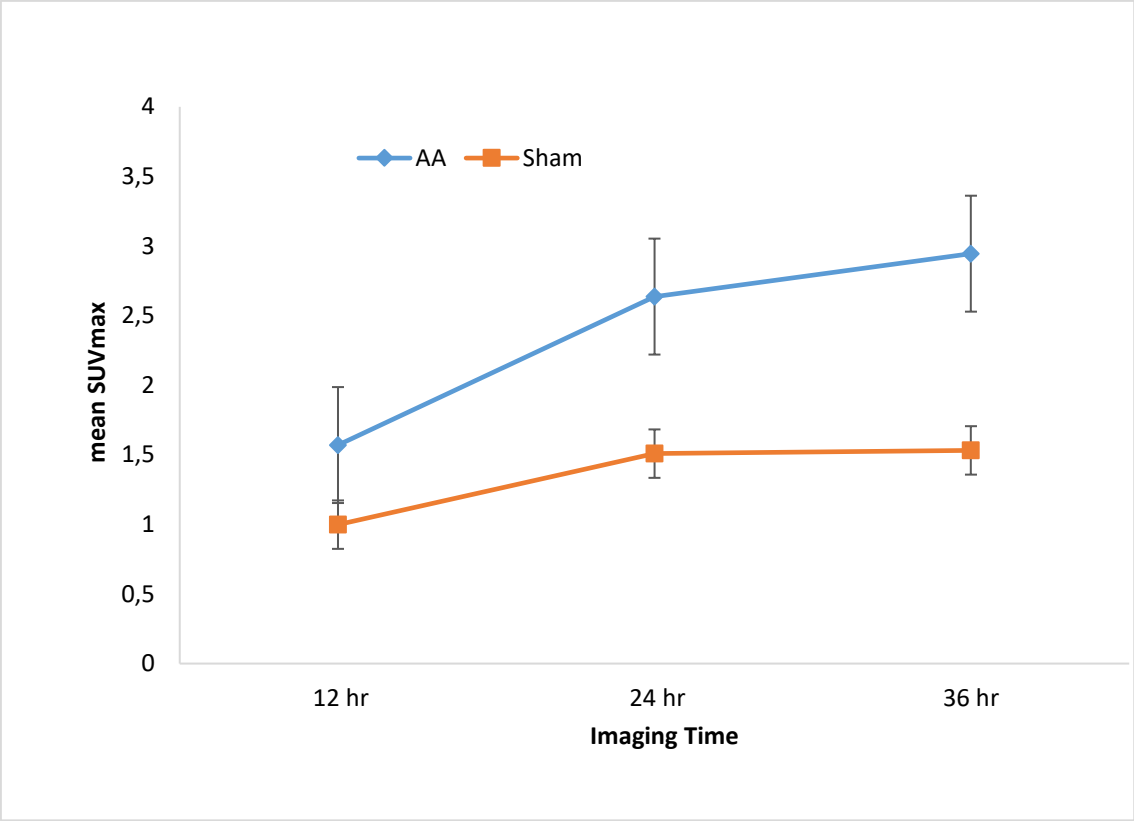

Fig. 4 ^{68}Ga-citrate PET/CT images, time graph of SUV_{max} averages obtained from AA region for the AA and sham group.

The most remarkable finding in the acquired ^{68}Ga-citrate PET/CT images in all rabbits is that the background involvement of ^{68}Ga was high in the abdominal region, whereas blood pool (BP) activity was particularly intensive in the heart and large vessels.

In the histopathological evaluation of the AA group, neutrophil infiltration and focal necrosis in all cases and complete necrosis in perforated and gangrenous cases were detected. Histopathologically, appendicitis findings were not observed in all rabbits in the sham group. Fig. 5 shows the histopathological features of the sham and AA groups.

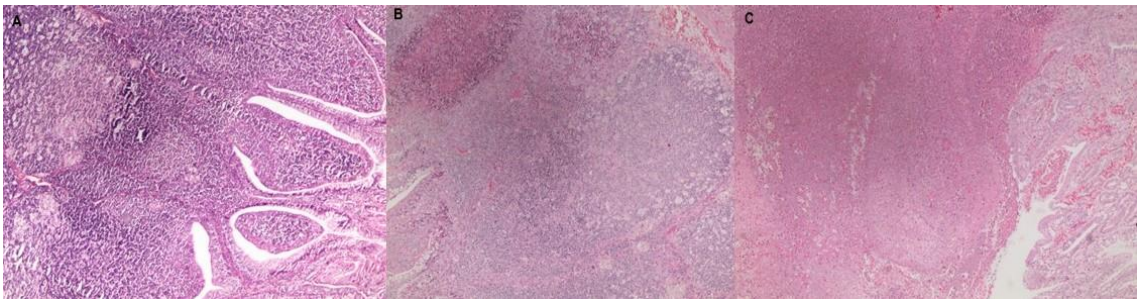

Fig. 5 Histopathological view of the appendix of a rabbit in the sham group (a) neutrophil infiltration of the mucosa and appendix wall (b) Histopathological examination of another rabbit in the AA group showed full-layer necrosis (c) in the appendix wall (HEX 40).

Procalcitonin and interleukin-6 levels

When comparing the results of the initial blood samples taken from the AA and the sham groups, no statistically significant differences in Pct were found. We found statistically significant differences in IL-6 levels between the two groups. In basal blood measurements, IL-6 levels in the AA group were significantly higher than those in the sham group. At 36 h, Pct and IL-6 levels in the AA group were significantly higher than those in the sham group. In the AA group, Pct and IL-6 levels were significantly higher at 36 h than at baseline. There was no statistically significant change in these levels in the sham group at 36 h compared with those at baseline. (Table 3-4).

Table 3 Procalcitonin (pg/mL) results

		0 h		36 h		
	Groups	Mean ± SD	Median (min–max)	Mean ± SD	Median (min–max)	P (in-group)
Pct	AA	13.73± 5.49	13.79 (4.45–19.56)	24 ± 11.09	23.97 (5.45–39.56)	0.027#
	Sham	6.56 ± 1.12	6.4 (5.47–8.52)	7.09 ± 1.4	6.86 (5.25–9.52)	0.168
	P(inter-groups)		0.065		0.041*	

p < 0.05, statistically significant difference; *Mann–Whitney U test; #Wilcoxon Paired test

Table 4 Interleukin-6 (pg/ml) results

		0 h		36 h		
	Groups	Mean ± SD	Median (min–max)	Mean ± SD	Median (min–max)	P (in-group)
Pct	AA	4.59 ± 1.47	4.8 (2.35–6.45)	10.62 ± 1.14	10.73 (8.98–12.15)	0.028#
	Sham	1.97 ± 0.18	2 (1.66–2.22)	2.29 ± 0.44	2.07 (1.94–3.01)	0.344
	P(inter-groups)		0.002*		0.002*	

$p < 0.05$, statistically significant difference; *Mann–Whitney U test; #Wilcoxon Paired test

Discussion

We synthesized ^{68}Ga-citrate by making modifications in the automatic and closed synthesis unit. The labelling efficiency of the final product was >98%, and its pH was between 4 and 5. We correctly obtained the ^{68}Ga-citrate peak using HPLC, and our findings are consistent with those of similar studies [26-29]. The most important advantage of our labelling method is that it occurs in a closed and automated system, thereby reducing the risk of microbiological contamination and radiation exposure of the personnel. Using this method, the synthesis time of ^{68}Ga-citrate is 15 min.

Our study is the first rabbit study in the literature to evaluate an experimental AA model with ^{68}Ga-citrate PET/CT. Previously, many nuclear medicine imaging methods have been attempted in clinical and pre-clinical studies of AA. However, none could achieve routine clinical use for AA. In this study, ^{68}Ga-citrate labelling, PET/CT and evaluation were completed within 2 h under emergency conditions. This time is much shorter than those of other molecular imaging methods.

By considering histopathological findings as the gold standard, we calculated the sensitivity, specificity and accuracy of ^{68}Ga-citrate PET/CT at 36th hour in rabbit appendicitis to be 100%, 83.3% and 91.6%, respectively. Turan et al [30] investigated the appendicitis imaging efficacy of ^{99m}Tc-citrate and ^{67}Ga-citrate by establishing an AA model similar to that established in our study. In their study, ^{99m}Tc-citrate accurately detected 87.5% of AA cases. Furthermore, ^{67}Ga-citrate accurately detected AA in 75% of cases. In a study investigating children with suspected AA, the same study group revealed that the ^{99m}Tc-citrate sensitivity, specificity and total accuracy were 78.9%, 90.9% and 83.3%, respectively [31]. Our results are better than those obtained using ^{99m}Tc-citrate and ^{67}Ga-citrate. In the study by Turan et al [30], no anatomical correlations were made. Therefore, it is difficult to interpret which anatomical region is involved in the uptake of ^{99m}Tc-citrate and ^{67}Ga-citrate in the abdomen. ^{68}Ga-citrate PET/CT images did not reveal ^{68}Ga-citrate uptake in the appendix wall, and non-focal, heterogeneous involvement was detected in the periappendicular region. The uptake level was moderate. We think that this led to an increase in ^{68}Ga-citrate uptake for two reasons. The first reason involves the inflammatory reaction in the periapendicular region, and the second involves the increased blood flow secondary to inflammation. In any case, the CT correlation clearly demonstrates that the appendix mass itself does not have ^{68}Ga-citrate uptake.

One of our cases (sham1) was also evaluated as FP. Histopathological examination revealed no evidence to explain this. We think that the reason for the FP may be the high BP activity in the abdomen or an infection secondary to the operation.

The current literature has highlighted a distinct involvement of ^{67}Ga and ^{68}Ga-citrate in intra-abdominal infections in two cases. In fact, the lesion/background ratio was very high in both cases and the Ga uptake was evident [32,33]. In our study, the lesion/background contrast was not as prominent, and no focal involvement was observed. This difference can be thought to be due to the different levels of infection and inflammation involved or because of different patterns of physiological distribution between rabbits and humans. In a prospective clinical study comparing ^{67}Ga and ^{68}Ga-citrate, the sensitivity of ^{68}Ga-citrate was found to be low in soft tissue infections, which occurred because of high BP activity in the mediastinum and abdomen [34]. In most infection and inflammation imaging studies performed using ^{68}Ga-citrate PET/CT, high BP activity has been shown to be the most critical issue. In fact, researchers have

indicated that ^{68}Ga-citrate was not useful in mediastinal and upper abdominal lesions because of high BP activity and physiological involvement in the liver, spleen and kidney. In our study, BP activity was a factor that made PET/CT evaluation difficult. In rabbits, the appendix is relatively large and is located in the medium-lower abdomen, similar to that in humans. Therefore, BP activity partially caused difficulties in evaluating AA in rabbits.

Acute-phase reactants are used as biochemical markers in the diagnosis of AA. In our study, Pct and IL-6 levels in rabbits in the AA group following appendectomy were significantly higher compared with those at baseline ($p > 0.05$). Furthermore, there was no significant difference in these values between the sham group and at baseline. Basal IL-6 levels were higher in the AA group than in the sham group, and basal blood samples were taken immediately following the establishment of the AA and sham models. Hence, this demonstrates that IL-6 begins to increase rapidly with the onset of inflammation, and our results are consistent with current literature findings [29]. Pct levels were not increased in patients with sterile inflammation or viral infection. Therefore, it remains a good biomarker in many inflammatory conditions such as AA, sepsis and meningitis. When both tests were concomitantly evaluated, the sensitivity and specificity values were 95% and 55%, respectively. It was reported that Pct and IL-6 are more efficient predictors of AA than IL-2 and D-dimer [23]. Our main aim when planning the study was to investigate the relationship between Pct and IL-6 levels and SUV_{max} values by acquiring blood samples at the same time with ^{68}Ga-citrate PET/CT imaging times. Unfortunately, we were unable to perform this evaluation because we could not obtain an adequate number of blood samples. However, we have also proved that inflammation occurs in rabbit AA models with biochemical parameters.

This study has several limitations. We were unable to use this imaging modality in real clinical cases because ^{68}Ga-citrate is not licensed for human use in our country. Second, our study is an experimental animal study, so the number of animals used was small. Pre-clinical and clinical trials assessing larger populations in the future will more clearly reveal the value of ^{68}Ga citrate in AA. The third limitation of our study was that the results of PET/CT imaging at 12 and 24 h could not be correlated histopathologically. Sensitivity, specificity and accuracy calculations were made only considering the findings at 36 h.

Conclusions

In our study, ^{68}Ga-citrate PET/CT showed AA with high sensitivity and specificity in rabbit models with experimental AA. Future studies conducted using real clinical cases should be performed.

Declarations

Ethics approval and consent to participate: Approval was obtained from the ethical committee of animal experiments at our university. European Union directives have been followed.
Ethics committee approval date and number: Jan 11, 2019-60758568-020/2717
Consent for publication: Not applicable

Availability of data and materials: Our availability of data and material statement is as follows:

The datasets used and/or analysed during the current study are available from the corresponding author on reasonable request.

All data generated or analysed during this study are included in this published article [and its supplementary information files].

Funding: Our research was supported by Pamukkale University (Denizli, Turkey) Scientific Research Projects Coordination Unit. Project support is provided for research only and no support is provided for any publication produced from the project.

Project decision date and number: Feb 05, 2019/1

Authors' contributions:

AG is the responsible author. He planned to work. He organized all the stages of the study. He wrote the manuscript.

OU is a pediatric surgery. He performed the surgical operations of the rabbits.

AU is a Radiochemist. Prepared radiopharmaceuticals and made quality controls

ND evaluated histopathological materials.

EA Performed biochemical analysis of blood samples.

DY is a nuclear medicine physician. He evaluated on PET/CT images of experimental animals. He did the last checks of manuscript.

Acknowledgements: The authors declare that they have no conflicts of interest. The authors would like to thank Enago (www.enago.com) for the English language review.

Competing interests: The authors declare that they have no competing interests.

References

1. Ferris M, Quan S, Kaplan BS, Molodecky N, Ball CG, Chernoff GW, Bhala N, Ghosh S, Dixon E, Ng S, Kaplan GG. The Global Incidence of Appendicitis: A Systematic Review of Population-based Studies. Ann Surg. 2017 Aug; 266:237-241.
2. Addiss DG, Shaffer N, Fowler BS, Tauxe RV. The epidemiology of appendicitis and appendectomy in the United States. Am J Epidemiol. 1990; 132:910–25.
3. Gorter RR, Eker HH, Gorter-Stam MA, Abis GS, Acharya A, Ankersmit M, et al. Diagnosis and management of acute appendicitis. EAES Consensus Development Conference 2015. Surg Endosc. 2016; 30: 4668-90.
4. Margenthaler JA, Longo WE, Virgo KS, Johnson FE, Oprian CA, Henderson WG, et al. Risk factors for adverse outcomes after the surgical treatment of appendicitis in adults. Ann Surg. 2003; 238:59–66.
5. Apisarnthanarak P, Suvannarerg V, Pattaranutaporn P, Charoensak A, Raman SS, Apisarnthanarak A. Alvarado score: Can it reduce unnecessary CT scans in the assessment of acute appendicitis? I'm J Emerg Med. 2015; 33: 266-70.
6. Nelson DW, Causey MW, Porta CR, McVay DP, Carnes AM, Johnson EK, et al. Investigation of clinical evaluation of the diagnosis of acute appendicitis and investigation of the confidence of the computed tomography. Am J Surg. 2013; 205: 452-6.
7. Shogilev DJ, Duus N, Odom SR, Shapiro NI. Diagnosis of appendicitis: Evidence-based review of the diagnostic approach in 2014. West J Emergency Med. 2014; 15: 859-71.

8. Wei PL, Tsai MC, Hung SH, Lee HC, Lin HC, Lee CZ. Risk of new-onset type II diabetes after appendicectomy. Br J Surg. 2015; 102:1267-71.
9. Stewart B, Khanduri P, McCord C, and others, Global disease burden of conditions requiring emergency surgery. Br J Surg. 2014; 101: 9-22.
10. Navarro DA, Weber PM, Kang IY, dos Remedios LV, Jasko IA, Sawicki JE. Indium-111 leukocyte imaging in appendicitis. AJR Am J Roentgenol. 1987 Apr;148(4):733-6.
11. Annovazzi A, Bagni B, Burroni L, D'Alessandria C, Signore A. Nuclear medicine imaging of inflammatory/infective disorders of the abdomen. Nucl Med Commun. 2005;26(7):657-64.
12. Ali SZ, Yin LH, Kin KL, Sinha AK, Poon LM. 18F-FDG PET/CT Scan Can Predate Clinical Presentation in Acute Appendicitis. Clin Nucl Med. 2017;42: e409-e411.
13. Toriihara A, Yamaga E, Nakadate M, Oyama J, Tateishi U. Detection of unexpected emergency diseases using FDG-PET/CT in oncology patients. Jpn J Radiol. 2017; 35:539-545.
14. Bourgeois S, Van Den Berghe I, De Geeter F. Incidental finding of silent appendicitis on (18)F-FDG PET/CT in a patient with small cell lung adenocarcinoma. Hell J Nucl Med. 2016; 19:164-6.
15. Oner AO, Boz A, Aydin F, Cevikol C. A case of plastron appendicitis mimicking malignant cecal tumor in flourodeoxyglucose-positron emission tomography/computed tomography study. Indian J Nucl Med. 2015; 30:256-8.
16. Vorster M, Buscombe J, Saad Z, Sathekge M. Past and Future of Ga-citrate for Infection and Inflammation Imaging. Curr Pharm Des. 2018;24(7):787-794.

17. Vorster M, Maes A, Wiele Cv, Sathekge M. Gallium-68 PET: A Powerful Generator-based Alternative to Infection and Inflammation Imaging. Semin Nucl Med. 2016; 46:436-47.
18. Roivainen A, Jalkanen S, Nanni C. Gallium-labelled peptides for imaging of inflammation. Eur J Nucl Med Mol Imaging. 2012; 39:68-77.
19. Lamps LW. Infectious causes of appendicitis. Infect Dis Clin North Am. 2010; 24: 995-1018.
20. Bhangu A, Søreide K, Di Saverio S, Assarsson JH, Drake FT. Acute appendicitis: modern understanding of pathogenesis, diagnosis and management. Lancet. 2015: 26; 386:1278-87.
21. Taylor R, Jones A, Kelly S, Simpson M, Mabey J. A Review of the Value of Procalcitonin as a Marker of Infection. Cureus. 2017;9:e1148.
22. Yamashita H, Yuasa N, Takeuchi E, Goto Y, Miyake H, Miyata K, et al. Diagnostic value of procalcitonin for acute complicated appendicitis. Nagoya J Med Sci. 2016; 78:79-88.
23. Destek S, Gül VO, Menteş MÖ, Çiçek AF. Diagnostic efficacy of serum procalcitonin, IL-6, IL-2, and D-dimer levels in an experimental acute appendicitis model. Turk J Gastroenterol. 2019; 30: 641-7.
24. Şimşek G, Sevinç B, Ünlü Y, Hasırcı İ, Kurku H, Karahan Ö. Effect of medical treatment on histological findings in rabbits with acute appendicitis. Ulus Travma Acil Cerrahi Derg. 2016;22:516-520.
25. https://www.ich.org/page/qualty-guidlines, accessed Dec 15,2019.

26. Rizzello A, Di Pierro D, Lodi F, Trespidi S, Cicoria G, Pancaldi D, et al. Synthesis and quality control of 68Ga citrate for routine clinical PET. Nucl Med Commun. 2009;30:542-5.

27. Jensen SB, Nielsen KM, Mewis D, Kaufmann J. Fast and simple one-step preparation of ^{68}Ga citrate for routine clinical PET. Nucl Med Commun. 2013 Aug; 34:806-12.

28. Vorster M, Mokaleng B, Sathekge MM, Ebenhan T. A modified technique for efficient radiolabeling of 68Ga-citrate from a SnO2-based 68Ge/68Ga generator for better infection imaging. Hell J Nucl Med. 2013; 16:193-8.

29. Aghanejad A, Jalilian AR, Ardaneh K, Bolourinovin F, Yousefnia H, Samani AB. Preparation and Quality Control of (68) Ga-Citrate for PET Applications. Asia Ocean J Nucl Med Biol. 2015; 3:99-106.

30. Turan C, Tutuş A, Ercan MT, Ozokutan BH, Yolcu T, Köse O, et al. Evaluation of 99mTc-citrate, 67Ga-citrate and 99mTc(V) dimercaptosuccinic acid for the scintigraphic visualization of acute appendicitis. Res Exp Med. (Berl).1997;197:157-64.

31. Turan C, Tutuş A, Ozokutan BH, Yolcu T, Köse O, Küçükaydin M. The evaluation of technetium 99m-citrate scintigraphy in children with suspected appendicitis. J Pediatr Surg. 1999; 34:1272-5.

32. Vijay Kumar, Dilip K. Boddeti, Scott G. Evans and Socrates Angelides. ^{68}Ga-Citrate-PET for Diagnostic Imaging of Infection in Rats and for Intra-Abdominal Infection in a Patient, Current Radiopharmaceuticals. 2012; 5: 71.

33. Segard T, Morandeau LMJA, Dunne ML, Robinson JO, Murray RJ, Geelhoed EA, et al. Comparison between gallium-68 citrate positron emission tomography-

computed tomography and gallium-67 citrate scintigraphy for infection imaging. Intern Med J. 2019; 49:1016-1022.

34. Haghi AR, Kasraianfard A, Monsef A, Kazemi AS, Rahimi S, Javadi SMR. The diagnostic values of procalcitonin and interleukin 6 in acute appendicitis. Turk J Surg. 2018; 20:1-3.

Figures

Figure 1

Establishment of the sham (a) and experimental models of AA (b). The red arrow indicates the region where the appendix was ligated

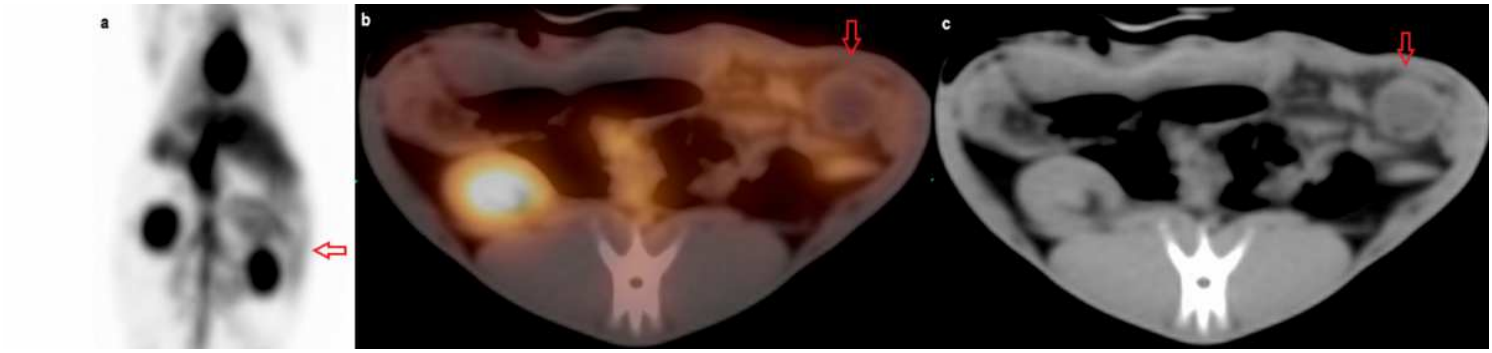

Figure 2

In 36-h 68Ga-citrate PET/CT images of a rabbit (AA6) with experimental acute appendicitis, acute appendicitis is observed in the abdomen adjacent to the left kidney and spleen. MIP (a); transaxial PET/CT fusion image (b); transaxial CT image (c) (red arrows).

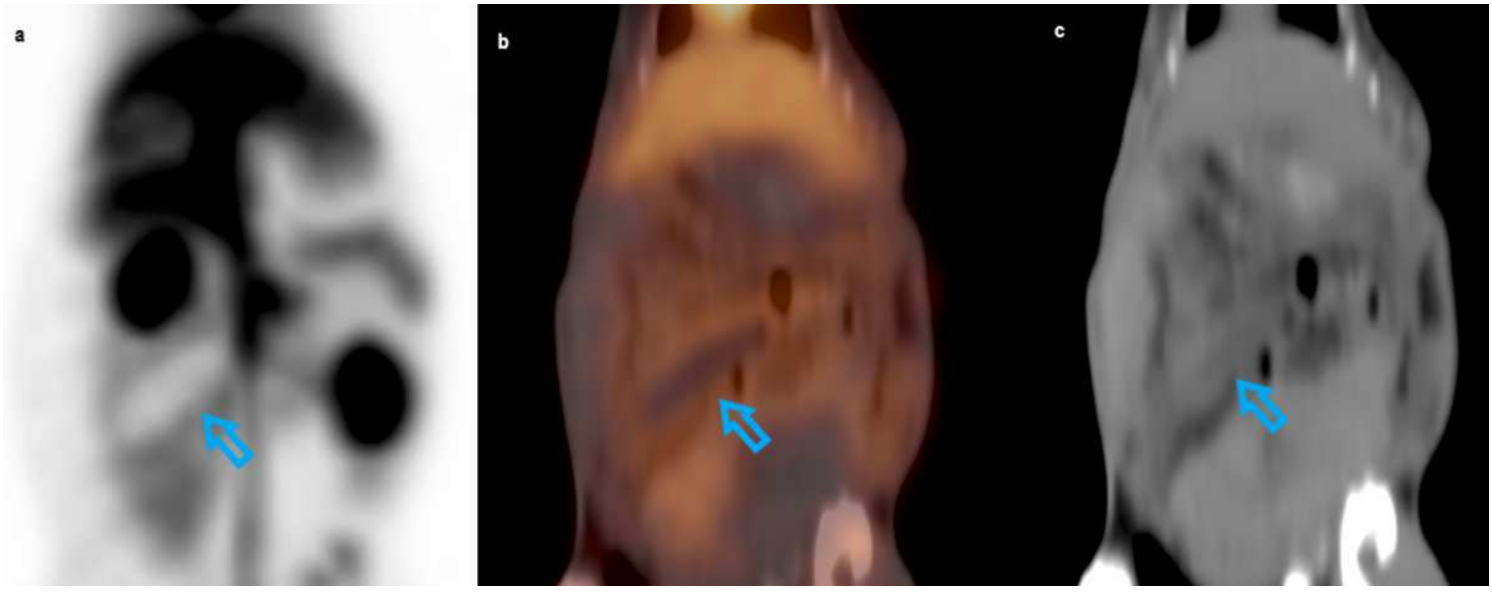

Figure 3

In 36-h 68Ga-citrate PET/CT images of a rabbit (AA4) with experimental acute appendicitis, acute appendicitis is observed in the abdomen in the right lower quadrant. MIP (a); PET/CT coronal fusion image (b);coronal CT image (c) (blue arrows).

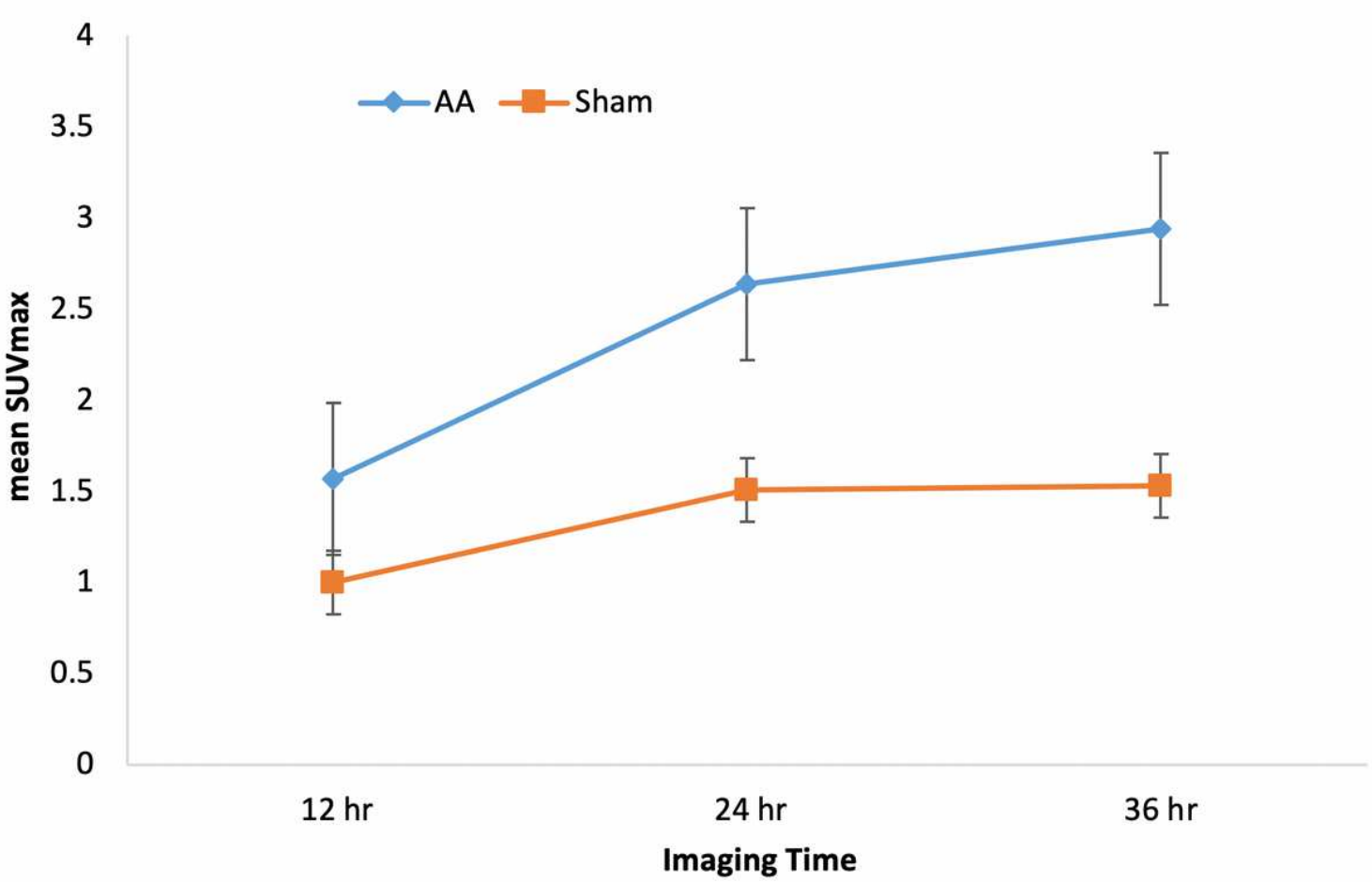

Figure 4

68Ga-citrate PET/CT images, time graph of SUVmax averages obtained from AA region for the AA and sham group.

Figure 5

Histopathological view of the appendix of a rabbit in the sham group (a) neutrophil infiltration of the mucosa and appendix wall (b) Histopathological examination of another rabbit in the AA group showed full-layer necrosis (c) in the appendix wall (HEX 40).